UNIVERSITY OF CALIFORNIA
RIVERSIDE

Modeling the Size Frequency Distributions of the Trilobite *Aulacopleura koninckii* and its Implications for Understanding Trilobite Biology and Preservation Potential

A Thesis submitted in partial satisfaction
of the requirements for the degree of

Master of Science

in

Geological Sciences

by

Rachel Lynn Kolenko

March 2016

Thesis Committee:
Dr. Nigel C. Hughes, Chairperson
Dr. Gareth Funning
Dr. Richard A. Minnich

The Thesis of Rachel Lynn Kolenko is approved:

_____

_____

_____

Committee Chairperson

Acknowledgements

Most importantly, I would like to thank my advisor, Dr. Nigel Hughes, for both his support and insight during my time as a graduate student. Thank you for helping me grow as a paleontologist and giving me the opportunity to investigate my research to the fullest extent.

I would like to acknowledge my other committee members, Dr. Gareth Funning and Dr. Richard Minnich for their input during the thesis writing process.

Many thanks also goes out to the friends I have made during my time at the University of California, Riverside for the unforgettable memories we created.

I would like to recognize the University of California, Riverside especially the Department of Earth Sciences for providing me with the means necessary to pursue my graduate education.

And finally, I would like to thank my family. Without their perpetual support I would not be where I am today.

ABSTRACT OF THE THESIS

Modeling the Size Frequency Distributions of the Trilobite *Aulacopleura koninckii* and its Implications for Understanding Trilobite Biology and Preservation Potential

by

Rachel Lynn Kolenko

Master of Science, Graduate Program in Geological Sciences
University of California, Riverside, March 2016
Dr. Nigel C. Hughes, Chairperson

Trilobites were a diverse group of Paleozoic marine arthropods, a group whose growth is characterized by exoskeletal ecdysis, or the molting of the outer cuticle. If all sclerites from all growth stages were preserved in a fossil assemblage, the distribution would be expected to be strongly right skewed because all individuals must have pass through smaller molt stages. While not all juveniles survive to large size, the overwhelming majority of observed trilobite size frequency distributions have normal distributions. This study investigates this disparity using a modified version of the method used by Hartnoll and Bryant (1990) to model crab size frequency distributions

based on the parameters of instar duration, mortality rate, sizer per instar, and number of instars. Here I apply this method to the trilobite *Aulacopleura koninckii*, a Silurian species whose growth is among the best known for any fossil, and for which size-specific assemblages of articulated individuals are recorded. This required a combination of parameters known for *A. koninckii*, in combination with other estimates based on living crab biology. Observed growth parameters from *A. koninckii* suggest that this trilobite underwent up to 33 post-potaspid instars separated by 32 post-potaspid molts. A range of low mortality rates, 5%, 10%, 15% at the first meraspid were assumed based on evidence that this taxon occupied a low predation environment. Assuming a constant recruitment and crab-based estimates of systematic changes in inter-molt duration, I was able to model predicted distributions of *A. koninckii* sizes that matched the largest individuals observed. Estimated life spans of *A. koninckii* according to these parameters ranged between 1 and 20 years. Although fitting the observed size range these distributions predicted far larger numbers of smaller specimens than larger ones, but this was not observed in the fossil record. To account for the dearth of smaller individuals, I explored the effect of selective preservation. Simulations suggest that the size frequency distributions observed for *A. koninckii* could be the outcome of either preservation bias against smaller trilobites or events that killed young populations.

Table of Contents

List of Figures

List of Tables

Introduction

Size frequency distribution plots are often used to report the occurrence of organisms in a single population or assemblage belonging to a single species. With regard to fossil data, a size frequency distribution can convey both biological and preservation data about a specific taxon, reflect variations among species that may indicate different life histories, and thus reveal aspects of paleoecological habits.

In trilobites, size frequency distributions are complicated by their molting habit. Rarely is it known whether fossil material represents fresh carcasses killed during burial, individuals dead prior to burial, or exuviae: the remains of the exoskeleton after molting. This study uses simulated models of arthropod growth, based on those of Hartnoll and Bryant, 1990, to explore different aspects of trilobite life history, constrained by our best knowledge of trilobite biology, and the use of reasonable comparison with living arthropods. Using these constraints I produced a range of size frequency distributions that are within plausible bounds for the trilobite, *Aulacopleura koninckii,* a species whose ontogeny and occurrence is well documented.

Background

To explore the possible controls of ancient size frequency distributions, it is necessary to constrain the varied inputs that could account for such distributions. This requires focusing on those species whose growth is well known. Many living arthropods grow according to Dyar's rule (1890), which is the observation that per-molt size increases occur at a constant growth increment (Fusco et al. 2012). Such a pattern of

growth is also evident among trilobites, with values of per-molt growth increments varying between 1.03 and 2.21 in the meraspid growth stages (Fusco et al. 2012). The growth increment of *A. koninckii* is particularly well constrained, due to the unusual site specific preservation of hundreds of articulated specimens spanning almost the full range of post-protaspid ontogeny; for total body length it is estimated as 1.12 (Hughes et al. 2014). During the meraspid period, in which segments accreted progressively in the thorax, it is possible to precisely determine individuals between instar (molt phase) growth increment, which are remarkably constant (Fusco et al. 2004). Furthermore, variance in size within instars is also notably constant (Fusco et al. 2004). The constant meraspid molt increment provides a justifiable basis of projecting into the following holaspid stage in order to estimate the number of molts required to account for the largest observed individual. The number was 32, with the longest individuals being about 28 millimeters in length.

Previous studies conducted by Hartnoll (1978), Sheldon (1988), and Hartnoll and Bryant (1990) explored various size distribution characteristics of fossilized trilobite and modern crab populations and accumulations. These were based on both observed growth and tempo of molting increments, i.e. the time interval between molts, under varied sea water temperature and salinities. Hartnoll (1978) also modeled the cumulative, standing size frequency distribution of a crab population based on a model that considered projected growth increments and molt tempo, at assumed constant recruitment and mortality. Surprisingly, Hartnoll (1978) showed from observed growth parameters that the size distributions of living crabs are predicted to be normal with high infant mortality.

As the rate of molting decreases, the numbers of individuals accumulate at given larger sizes or instar numbers.

Hartnoll and Bryant (1990) built on Hartnoll's previous work by modeling the frequency distributions, both instar and size, of decapod populations. They used the parameters instar duration, mortality, and average carapace width per instar to produce frequency distributions for crab species *Cancer anthonyi*. They modeled 4 different types of distributions; the population of live crabs, the number of corpses, the exuviae produced, and a combination of exuviae and corpses. Hartnoll and Bryant (1990) found that the frequency distributions of live populations of crabs differed markedly from the distributions of their corpses, exuviae, and the mixture of both corpses and exuviae (Figure 1).

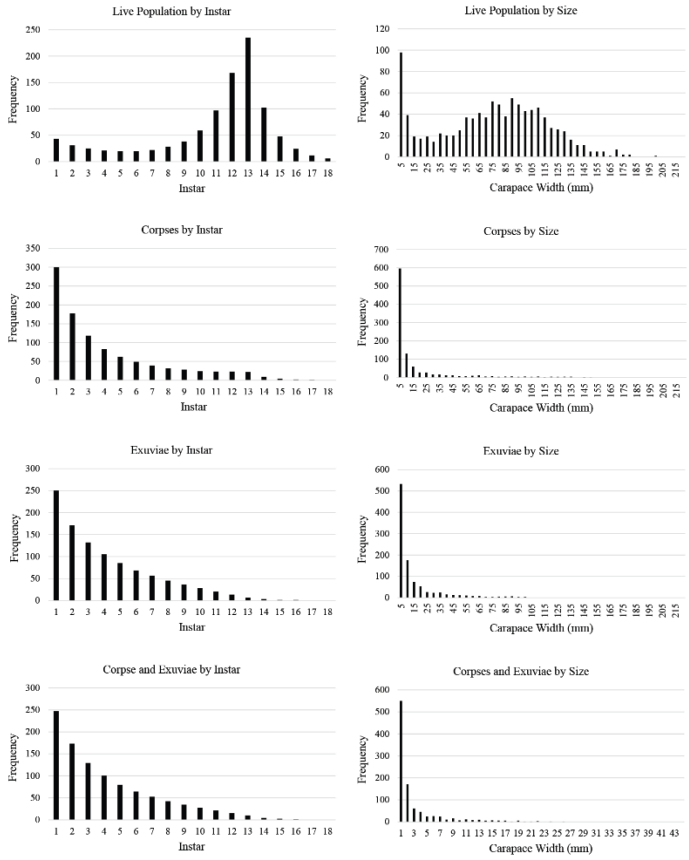

Figure 1: Frequency distributions by instar (left column) and size (right column) from Hartnoll and Bryant, 1990

As determined previously, distributions of live individuals had a normal distribution due to each subsequent intermolt period in an organism's life cycle being longer in duration than the previous intermolt. This caused a population in equilibrium to have a normal distribution as individuals from multiple cohorts/ generations pooled at the larger instars. The three remaining distributions have a right skew, reflecting the accumulated remnants of the crab populations, rather than the profile of an assemblage of living animals. The corpses-only distribution is right skewed because there are more crabs initially at the lower instars. Thus there are more crabs to become victims of the

model's mortality rate (i.e. 15% mortality of 1000 crabs is 150, while 15% of 100 crabs is 15). Similarly, a right skew distribution is also seen among exuviae because larger numbers of individuals were present at the smaller instars, each one contributing their molts to the accumulation. The gradual decrease in the number of molts also reflects the reduced number of crabs at each subsequent instar. Assuming complete preservation, the nature of the materials accumulating may be reflected in the type of distribution observed.

While Hartnoll and Bryant's (1990) instar durations and size data were based on data collected from live crabs, they also needed to estimate the overall mortality rate at each instar. Since natural mortality rates are difficult to determine, an equation was used to project mortality based on both instar duration and the number of instars for the species based on earlier work by Anderson and Ford (1976) (see below). The equation employed two mortality rates to calculate total mortality per instar. The first rate was kept constant and represented the mortality at each instance of ecdysis: molting of the outer cuticle. The second rate calculated the intermolt mortality at each instar. This value varied based on the duration of each instar. The instars with longer durations had higher mortalities due to individuals spending more time in those instars. Hartnoll and Bryant (1990) found this equation accurately predicts the observed mortality rate of their crab populations at each instar in their development and assumed a relatively low starting mortality rate of 30% (15% at ecdysis and 15% during the intermolt period).

Anderson and Ford (1976) evaluated growth in *Cancer anthonyi*, a crab species with a maximum carapace width of 165 mm and reaches maturity after 10-12 molts.

Raising crabs from eggs to death, they recorded the durations of each instar and its size, and defined a relationship that projects size and duration at each instar. Both size and instar duration observed in juveniles could be extrapolated to predict these parameters for later instars when assuming ideal conditions.

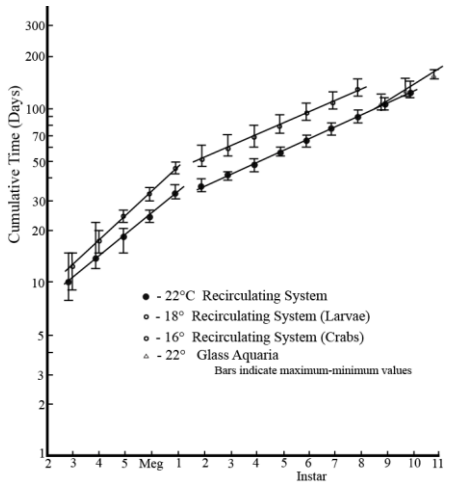

Figure 2: Graph used in Anderson and Ford (1976) to derive instar duration equation (equation 1 in this paper).

Instars plotted based on cumulative time in days on a log plot, permitted the extrapolation of instars to obtain reasonable estimates for their durations of those instars (Figure 2 and Equation 1). Anderson and Ford (1976) found that extrapolating their modeled data was within a few days of the empirical data.

Sheldon (1988) examined the size frequency distributions of species belonging to several trilobite genera collected as part of a substantial study of trilobite microevolution. He plotted size frequency distributions of each species within and among stratigraphic section. Sheldon (1988) found that the majority of plotted distributions had a normal

distribution. Normal distributions were also most common among articulated trilobites, and may reflect a stable population in the fossil record, but underlying causes are unclear. Hartnoll and Bryant (1990) expanded upon Sheldon's findings by showing what assemblages comprised the exuviae and corpses accumulated from standing populations looked similar.

Normal distributions for trilobite assemblages have been recorded in the literature. Examples include *A. koninckii* (Hughes et al., 2014), which calculated size frequency of individual fossil beds at Na Cernidlech Hill in the Czech Republic. Feist et al. (Figure 7, 2008) collected individuals from the trilobite, *Acuticryphops auceticeps* from the Virgin Hills Formation which plotted as a normal distribution with distinction peaks thought to indicate instars. Karim and Westrop (Figure 10, 2002) plotted normal size frequency distributions for two horizons of trilobite 'clusters' of the species *"Homotelus" bromidensis*. The first horizon is composed of carcasses only while the second was made up of exuviae and corpses.

Modern Arthropods

To constrain the parameters to be used for estimating trilobite size frequency distributions, records from modern arthropods were examined for durations, mortality rates, size per instar, and number of instars. Literature on modern decapod, isopod, and amphipod growth and development was consulted to constrain reasonable parameter estimates for trilobites. This review revealed limited information on the growth schedules of modern arthropods. Natural arthropod growth in nature is dependent on

parameters that are difficult to replicate in the laboratory and these can affect the maximum size attained by individuals and the speed of development. The information on marine arthropod growth is limited because of the difficulty in tracking organisms that shed their outer cuticle upon growth.

Recurrent trends are difficult to discern due to a wide variety of life modes and sizes. Small species of marine arthropod tend to reproduce once a year, usually in the late spring/ early summer, and develop quickly due to their short life spans of 1-2 years e.g., isopod species such as *Idotea baltica* (Strong and Daborn, 1979), and amphipod species such as *Gammarus wilkitzkii* (Poltermann, 2000). Larger arthropods tend to have longer life spans, although these do not necessarily develop through a large number of instars (i.e. many of these organisms have larger Dyar's coefficients). They tend to have maximum inter-molt periods of either one or two years in those with indeterminate growth (i.e., growth that is not terminated after a period of time or when some pre-determined biological attribute has completely developed [Hartnoll, 1982]). Some molt yearly upon reaching adulthood while others molt once per year upon adulthood, and then eventually transition to molting every other year (Carmichael et al., 2003 and Hartnoll and Bryant, 1990).

Aulacopleura koninckii

Aulacopleura koninckii's ontogeny is well known compared to other trilobites. Unusually large numbers of articulated specimens that span a wide range of post-protaspid sizes were found at Na Cernidlech Hill, near Lodenice in the Czech Republic

(Hughes et al. 2014). In this study we consider only those instars after the protaspid stage – i.e. after a functional articulation has appeared between the cephalic region and the developing trunk (see Hughes et al., 2006). This means that both embryonic and early hatching growth is not considered in our modeling. The geological setting was on the flank of a volcanic arc likely with fluctuating bottom-water oxygenation.

The 1.4 meter interval contain the articulated specimens of more than an hundred bedding surfaces upon which fossil material accumulated. Some surfaces comprise diverse assemblages of skeletonized Silurian organisms that include relatively few *A. koninckii*; others are largely monospecific accumulations of *A. koninckii*. These variations in abundance appear to be related to variable levels of bottom water oxygenation, with *A. koninckii* being an opportunistic species that apparently thrives at times of reduced oxygen availability (Hughes et al., 2014). The specimens of *A. koninckii* show a variety of articulation styles, suggesting that not all were alive at burial (Hughes et al. 2014). Mass mortality followed by burial might reflect fatal oxygen levels.

This kind of opportunistic life style suggests that *A. koninckii* may have grown quickly compared to other arthropods developing through multiple instars in a highly regular fashion. Rapid growth is necessary, in a fluctuating environment, to reach reproductive viability within a short period. On the other hand, life in a physiologically stressed environment could be expected to place severe constraints on organismal form, i.e., only those individuals precisely suited to the challenging physical conditions might be viable.

Materials and Methods

This study expands upon earlier research using precise data for *A. koninckii* that constrains several parameters required for modeling frequency distributions. The Hartnoll and Bryant (1990) and Anderson and Ford (1976), model used herein employs the following variables: molt tempo, mortality rate per instar, the average size of individuals at each instar, and the standard deviation in size at any particular instar. For consideration of the fossil record, two additional variables were added: preservation potential for exuviae and corpses. Hartnoll and Bryant's (1990) table was recreated in Microsoft Excel and values derived from empirical studies of *A. koninckii* substituted. The capacity of Excel was too limited to handle the large volume of numbers generated by this method (thousands per run). I wrote a program using Javascript, HTML, and CSS in the application building framework, Node Webkit, recently renamed NW.js (MIT, 2015). The mathematical basis for the models was written using Javascript while HTML and CSS were used to create the user interface for the program (input boxes for variables, background colors). Once this portion was completed, a graphing API was added to observe the generated distributions directly within the program. Google Visualization API (application programming interface; Google, 2015), a software development component package that can generate interactive graphs, was implemented for this step. Results are exportable via a text file and the program allows for 40 runs at once while varying one of the chosen variables (stage duration, mortality, minimum size, or Dyar's constant).

The number of instars and their average sizes was known from data obtained with 33 post-protaspid instars present (0-32) projected to be present based on the known Dyar's coefficient and the maximum observed specimen length. This number of molts, coupled with the relative small size of the largest *A. koninckii* (28 mm) imposes some constraints on the estimation of other parameters. For example, to achieve so many molts with relatively small size increments between them limits the rate of molting, particularly in the earliest stages of ontogeny. Using the methods of Anderson and Ford (1976), spreadsheets were constructed to test a large range of possible values based on equations one and two. The duration of each instar was calculated based on equation 1 used (Anderson and Ford, 1976) to forward calculate the durations of additional instars.

$$\log_e [\text{predicted time in days to instar}] = c + d[\text{instar number}]$$

Where variables c and d are derived from the formula for the exponential trend line when instar number is plotted against the cumulative time (in days) an individual is alive. The formula for the exponential trend line is $Y= ce^{bx}$, where in equation one variable c is equal to variable c in the exponential trend line equation and d is equal to e^{bx}. The equation for this line is derived from a graph that plots instar number against cumulative days an individual is alive on a log scale axis (see Figure 2). Equation one results in the cumulative days after hatching until an individual reaches that instar. While the total number of instars is known for *A. koninckii*, the other two variables are unknown. Therefore a wide range of possible values was explored (c = 0.1-3 and d=.001-0.14) to see what a species with 33 instars would have for instar durations and

under what range of values it was possible to produce individuals with 33 instars that reached the maximum observed size.

These calculations were run and summarized in spreadsheets based on three different types of lifespan modes. The first spreadsheet calculated the durations of each instar based on the premise of an increasing instar duration throughout growth, a trait generally observed in short-lived arthropods that live less than a year (e.g. the isopod; *Cirolana imposita* [Shafir and Field, 1980]). The second spreadsheet again calculated variable instar durations but once duration reached 365 days, instars were restricted to 365 day interval maximum, e.g. the horseshoe crab, *Limulus polyphemus*, before reaching its terminal molt (Carmichael et al. 2003). This reflects the yearly molt pattern of many marine arthropods. A third spreadsheet kept the increment constant at 365 days for instars until the project stage duration was between 365 and 730 days. After the projected durations pass 730 days, molt duration switched to 730 days. This simulates how some large species ultimately switching to a 2 year instar duration, after previously spending some of their instars at the 365 day limit (e.g. decapod, *Cancer anthonyi* [Anderson and Ford, 1976]).

Following the calculation of instar duration, the mortality was considered using equation 2 implemented by Hartnoll and Bryant (1990):

$$\%\ \text{Intermolt Mortality}_{(\text{instar n})} = \%\ \text{Intermolt Mortality}_{n=1} \times \frac{\text{CW}_{n=1}}{\text{CW}_n} \times \frac{\text{duration}_n}{\text{duration}_{n=1}}$$

CW is defined as carapace width at each instar in this equation. For *A. koninckii* I substituted the average total length per instar for this variable. Two different mortalities are calculated and then summed to get the total mortality at each instar. The first mortality rate used to calculate the total mortality is the mortality during ecdysis. This is an assigned rate and is constant at each occurrence of ecdysis, e.g. mortality at ecdysis is maintained at 5% whether it is the first molt modeled or the 31st. The second mortality is the intermolt mortality and is calculated using equation two. This is the mortality rate that the population experiences between molts. In equation two, an assigned mortality at instar one is used to calculate the intermolt mortality by multiplying the percentage intermolt mortality at instar one by the quotient of the carapace width at instar one by the carapace width at the current instar and the quotient of the instar duration at the current instar by the instar duration at instar one. As instar duration varies with size, so also the intermolt mortality varies through ontogeny.

Based on the model results in the spreadsheets, I determined whether each series of durations and mortality rates were plausible given other knowledge of the biology of *A. koninckii*. Some iterations could quickly be discounted when equation 1 was calculated due to unrealistic durations, e.g. durations with total life span exceeding 20 years. Iterations were also omitted from further consideration, because of issues related to initiation of the model following larval development. Equation one does not intercept the y-axis at instar zero because it takes into account time spent in an egg/ larval, and protaspid stage before the organism starts growing through meraspid instars. If the intermolt duration calculated for instar zero were notably different from the durations of

the early instars that model was omitted (e.g. if the organism were to spend 100 days in the initial stages but the duration of its meraspid instar zero was a day or less, this was clearly an unreasonable estimate). Any model that had a mortality rate that reached more than 100% before the 33rd instar could automatically be discarded. Based on modern arthropod life expectancies it was decided that a lifespan of over 20 years would be highly improbable based on the size and biological characteristics and environment of *A. koninckii*. From these parameters the results were narrowed down to areas where the potential biological parameters of *A. koninckii* appeared to be reasonable. A modeled frequency distribution did not reach close to the maximum number of instars (33), it could be discarded on the basis of failing to fit observed data. Many data series' could also be discarded based on their high mortality due to long intermolt periods.

This process allowed the definition of ranges for each of the lifespan-style spreadsheets, size data and their standard deviations were applied to the models to calculate the size frequency distributions of the population. The program calculated average size per instar using one of two methods, depending on the available data. The first way was by directly entering average size data per instar. The second method projected the average size for subsequent instars using the average size of the first instar and the observed Dyar's constant to extrapolate the size of the next instar by multiplying the average size of the previous instar by the Dyar's constant of the species. As the observed fit to Dyar's rule is extremely strong in *A. koninckii* these two methods are projected to yield similar results. Using the average size of the trilobites at each stage and its standard deviation, the program then calculated a distribution of random sizes for

each instar. The script takes the average size of trilobites at that stage and the standard deviation of the size at each stage then calculates random distributions within these bounds to achieve a normal distribution of values around the average. The number of random estimates made for each instar is based on the number of individuals per instar calculated in the preceding steps. These distributions were then plotted using the Google Visualizations API (Google, 2015). The API auto-bins the data based on the size data (specific size bins can be selected) and graphs a size frequency distribution.

If size frequency distributions that resulted from this modeling did not match those observed in the Na Cernidlech site in every case, the additional parameter of selective preservation was introduced to adjust the numbers of individuals in particular stages in an attempt to better mimic observed size frequency distributions. These preservation values do not affect the underlying model but rather served to selectively remove a proportion of each stage. This approach explores what kinds of preservational bias would be necessary to bring modeled size frequency distributions into accordance with that observed, to explore preservational biases.

Results

Results are presented based on the growth of *A. koninckii* with 33 projected post-protaspid instars under three possible life style modes (continuous increase in instar duration, continuous increase up to 365 day maximum, and 730 day maximum) applied under three mortality regimes (5%, 10%, and 15%), and also with an imposed modeled preservation bias.

Potentially Viable Lifespans

A wide range of possible growth exponentials required exploration because the duration of trilobite instars is unknown, and the results have been compiled in figures 3-5. The horizontal axis represents a range of variables input for variable D for equation 1 and the vertical axis represents the range of variables input for variable C for equation 1. From these the instar durations and their corresponding mortalities were calculated using equations 1 and 2. The mortality rates for each series were calculated using a 5% rate for the first meraspid instar, as this would yield the largest area of viable life spans compared 10% and 15% rate experiments. Each series of instar durations was then summed to obtain a life span which is displayed in each cell of figures 3-5. The three charts identify potentially viable combinations under the constraints that (1) any instar may not have a mortality of over 100% and (2) have a total lifespan of over 20 years, which is deemed unreasonable for an arthropod less than up to length of 30 mm that likely lived in fluctuating environmental conditions. The individual colors represent lifespan totals binned in 5 year increments.

As expected a larger molt increment yields longer lifespans, as observed in the progression from figures 3 to 5. As overall instar duration increases, the 20 year maximum can be approached quite rapidly with only a relatively modest increase in intermolt period per instar due to *A. koninckii*'s notably large number of post-protaspid instars.

	0.01	0.015	0.02	0.025	0.03	0.035	0.04	0.045	0.05	0.055	0.06	0.065	0.07	0.075	0.08	0.085	0.09	0.095	0.1
0.1	3	4	6	8	12	18	26	38	56	82	120	176	257	376	550	803	1175		
0.2	3	5	7	11	15	23	33	48	71	104	151	221	324	473	692	1012	1479		
0.3	4	6	9	13	19	29	42	61	89	130	191	279	407	596	871	1274	1862		
0.4	5	8	11	17	25	36	52	77	112	164	240	351	513	750	1097	1603	2344		
0.5	7	10	14	21	31	45	66	97	141	207	302	442	646	944	1380	2018	2951		
0.6	9	12	18	27	39	57	83	122	178	260	380	556	813	1189	1738	2541	3715		
0.7	11	16	23	33	49	72	105	153	224	327	479	700	1023	1496	2188	3199	4677		
0.8	13	20	29	42	62	90	132	193	282	412	603	881	1288	1884	2754	4027	5888		
0.9	17	25	36	53	78	114	166	243	355	519	759	1109	1622	2371	3467	5070			
1	21	31	46	67	98	143	209	306	447	653	955	1396	2042	2985	4365	6383			
1.1	27	39	58	84	123	180	263	385	562	822	1202	1758	2570	3758	5495				
1.2	34	50	72	106	155	226	331	484	708	1035	1514	2213	3236	4732	6918				
1.3	43	62	91	133	195	285	417	610	891	1303	1906	2786	4074	5957					
1.4	54	79	115	168	245	359	525	767	1122	1641	2399	3508	5129						
1.5	68	99	145	211	309	452	661	966	1413	2065	3020	4416	6457						
1.6	85	124	182	266	389	569	832	1216	1778	2600	3802	5559							
1.7	107	157	229	335	490	716	1047	1531	2239	3273	4786	6998							
1.8	135	197	288	422	617	902	1318	1828	2818	4121	6026								
1.9	170	248	363	531	776	1135	1660	2427	3548	5188									
2	214	313	457	668	977	1429	2089	3055	4467	6531									
2.1	269	394	575	841	1230	1799	2630	3846	5623										
2.2	339	495	724	1059	1549	2265	3311	4842	7080										
2.3	427	624	912	1334	1950	2851	4169	6095											
2.4	537	785	1148	1679	2455	3589	5248												
2.5	676	989	1445	2114	3090	4519	6607												
2.6	851	1245	1820	2661	3891	5689													
2.7	1072	1567	2291	3350	4898	7161													
2.8	1349	1972	2884	4217	6166														
2.9	1698	2483	3631	5309															
3	2138	3126	4571	6683															

Figure 3: Potential lifespans (in days) for *A. koninckii* if a constant increase in instar duration is applied. The vertical axis was down sampled to a .1 increment. Figure 6-8 and data simulations were run based on a .02 increment.

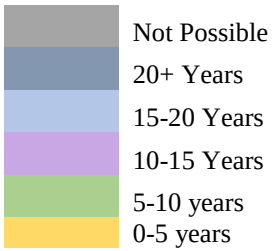

	0.025	0.03	0.035	0.04	0.045	0.05	0.055	0.06	0.065	0.07	0.075	0.08	0.085	0.09	0.095	0.1	0.105	0.11	0.115	0.12	0.125	0.13	0.135	0.14
0.1																								
0.2																								
0.3																								
0.4														2271	2873	3410								
0.5														2680	3259	3775	4253							
0.6													2448	3082	3645	4140	4599	4999	5364	5698				
0.7												2185	2873	3485	4031	4505	4945	5333	5683	6004	6299	6572	6824	7042
0.8												2636	3001	3888	4416	4870	5291	5668	6004	6312	6597	6855	7085	
0.9											2360	3090	3731	4293	4799	5235	5637	6002	6326	6623	6888	7128		
1											2844	3549	4162	4698	5181	5600	5983	6330	6641	6920	7173			
1.1										2553	3334	4010	4597	5105	5564	5965	6330	6659	6954	7220				
1.2										3074	3820	4461	5023	5512	5947	6330	6677	6989	7269					
1.3									2764	3598	4304	4915	5449	5921	6330	6695	7024							
1.4									3330	4116	4794	5374	5877	6330	6713	7060								
1.5								2995	3887	4644	5280	5835	6308	6732	7097									
1.6								3607	4455	5159	5764	6286	6740	7135										
1.7							3249	4214	5010	5684	6254	6740	7173											
1.8							3913	4820	5576	6203	6740	7199												
1.9						3527	4579	5432	6133	6724	7224													
2						4257	5245	6039	6697	7248														
2.1					3832	4987	5905	6645	7257															
2.2					4643	5717	6567	7257																
2.3					5456	6447	7231																	
2.4				5076	6270	7177																		
2.5				5992	7078																			
2.6			5562	6901																				
2.7			6606																					
2.8		6100																						
2.9																								
3	6675																							

Figure 4: Potential lifespans (in days) for *A. koninckii* if a 365 day maximum instar duration is applied. The vertical axis was down sampled to a .1 increment. Figures 6-8 and data simulations were run based on a .02 increment. See figure 3 for color key.

	0.01	0.015	0.02	0.025	0.03	0.035	0.04	0.045	0.05	0.055	0.06	0.065	0.07	0.075	0.08	0.085	0.09	0.095	0.1
0.1																			
0.2																			
0.3																			
0.4																			
0.5																			
0.6																			
0.7																	3850	5126	
0.8																	4618	5876	7060
0.9																4461	5752	6623	
1															3914	5257	6523		
1.1															4740	6057	7295		
1.2														4185	5556	6848			
1.3														5034	6375				
1.4													4481	5889					
1.5													5374	7105					
1.6												4820	6619						
1.7												5740							
1.8											5185	7036							
1.9											6527								
2										5610									
2.1										7000									
2.2									6082										
2.3																			
2.4								6635											
2.5																			
2.6							7266												
2.7																			
2.8																			
2.9																			
3																			

Figure 5: Potential lifespans (in days) for *A. koninckii* if a 730 day maximum instar duration is applied. The vertical axis was down sampled to a .1 increment. Figure 6-8 and data simulations were run based on a .02 increment. See figure 3 for color key.

Viable Lifespans

Once areas consistent with *A. koninckii*'s observed maximum number of molts and modeled growth function were determined (Figures 3-5), other mortality rates were then considered. Values of 10% and 15% mortality at the first meraspid instar, with intermolt mortalities changing thereafter in proportion to duration were explored. Results are shown in figures 6-8, cells within the red outline have at least one size frequency distribution of the four calculated (live population, corpses, exuviae, mixture of corpses and exuviae) under a 5% first meraspid mortality regime, reach the maximum number of instars. Those within the blue border represent life spans that could reach the maximum number of instars under a 10% first meraspid mortality regime and those within the green border represent those that were viable with a 15% instar first meraspid regime. A 'viable' lifespan in figures 6-8 had no mortality rate over 100% for any instar, spent 30 days or less in a protaspid/ larval stage, and a total life span of greater than 50 days. Protaspid/ larval stages that were greater than 30 days were excluded due to their implausibly high values with respect to the initial meraspid instar duration. For example, it is unlikely that *A. koninckii* would have spent more than a month in its protaspid stage if its total life span model's span was between 0-5 years. Total life spans that were less than 50 days show relatively little variation among instar durations, which results in the majority of *A. koninckii*'s instar durations being less than one day, which is unrealistic and not seen among modern marine arthropods. Figure 7 shows possible lifespans under a 365 day maximum instar duration. In addition to reaching all 33 instars, a lifespan must reach a 365 day duration in at least one instar, and spend less than 30 days in the

protaspid and larval stages. In figure 8, the same parameters for mortality and protaspid/ larval stage duration must be met but the lifespan must also reach an instar duration of 730 days for at least one instar. Colored borders in figures 6-8 represent the possible life spans under the 3 different mortality regimes. The red border denotes viable lifespans under a 5% meraspid one mortality, blue, 10% mortality at instar one, and green represents those possible under a 15% mortality at the initial meraspid instar

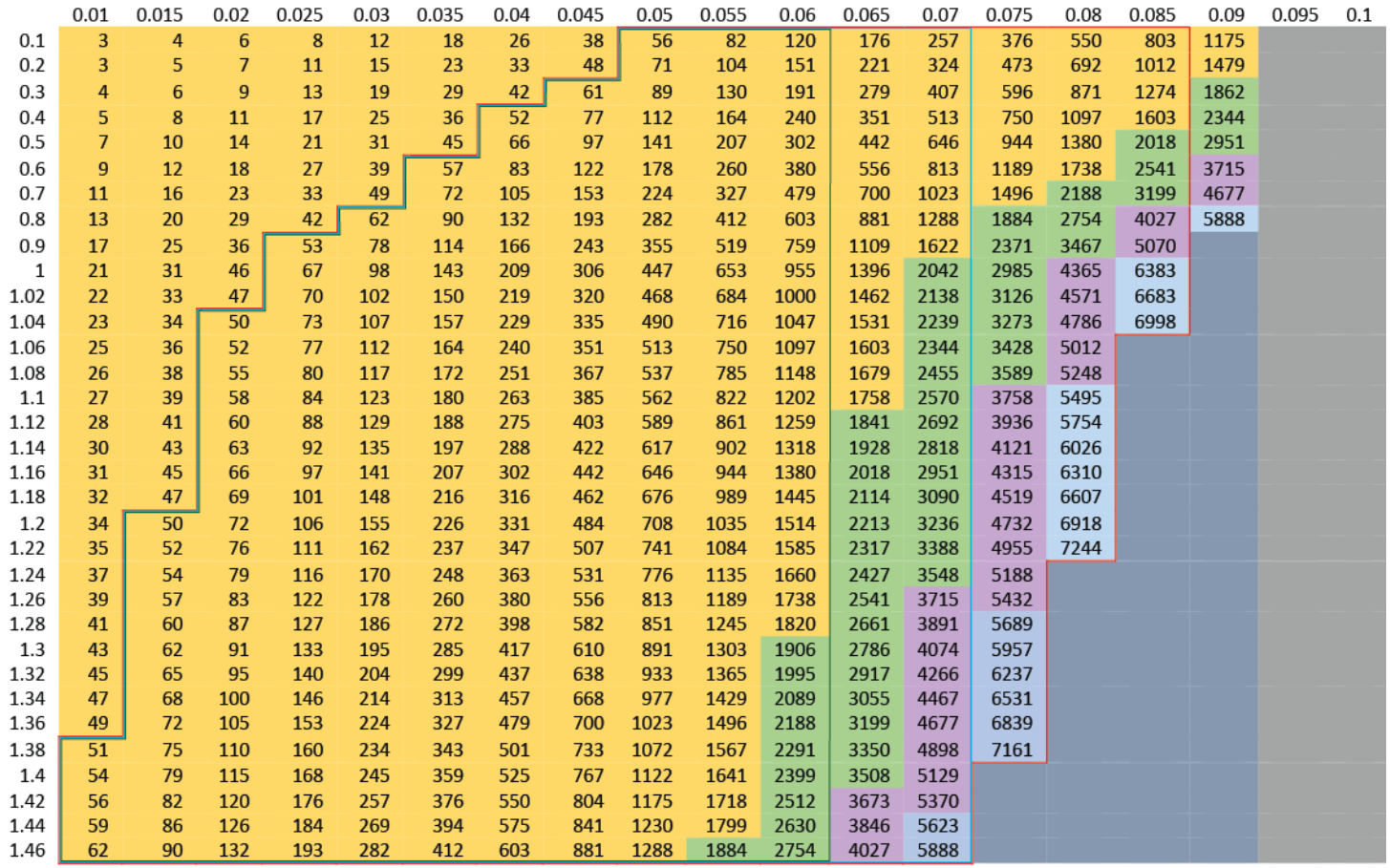

	0.01	0.015	0.02	0.025	0.03	0.035	0.04	0.045	0.05	0.055	0.06	0.065	0.07	0.075	0.08	0.085	0.09	0.095	0.1
0.1	3	4	6	8	12	18	26	38	56	82	120	176	257	376	550	803	1175		
0.2	3	5	7	11	15	23	33	48	71	104	151	221	324	473	692	1012	1479		
0.3	4	6	9	13	19	29	42	61	89	130	191	279	407	596	871	1274	1862		
0.4	5	8	11	17	25	36	52	77	112	164	240	351	513	750	1097	1603	2344		
0.5	7	10	14	21	31	45	66	97	141	207	302	442	646	944	1380	2018	2951		
0.6	9	12	18	27	39	57	83	122	178	260	380	556	813	1189	1738	2541	3715		
0.7	11	16	23	33	49	72	105	153	224	327	479	700	1023	1496	2188	3199	4677		
0.8	13	20	29	42	62	90	132	193	282	412	603	881	1288	1884	2754	4027	5888		
0.9	17	25	36	53	78	114	166	243	355	519	759	1109	1622	2371	3467	5070			
1	21	31	46	67	98	143	209	306	447	653	955	1396	2042	2985	4365	6383			
1.02	22	33	47	70	102	150	219	320	468	684	1000	1462	2138	3126	4571	6683			
1.04	23	34	50	73	107	157	229	335	490	716	1047	1531	2239	3273	4786	6998			
1.06	25	36	52	77	112	164	240	351	513	750	1097	1603	2344	3428	5012				
1.08	26	38	55	80	117	172	251	367	537	785	1148	1679	2455	3589	5248				
1.1	27	39	58	84	123	180	263	385	562	822	1202	1758	2570	3758	5495				
1.12	28	41	60	88	129	188	275	403	589	861	1259	1841	2692	3936	5754				
1.14	30	43	63	92	135	197	288	422	617	902	1318	1928	2818	4121	6026				
1.16	31	45	66	97	141	207	302	442	646	944	1380	2018	2951	4315	6310				
1.18	32	47	69	101	148	216	316	462	676	989	1445	2114	3090	4519	6607				
1.2	34	50	72	106	155	226	331	484	708	1035	1514	2213	3236	4732	6918				
1.22	35	52	76	111	162	237	347	507	741	1084	1585	2317	3388	4955	7244				
1.24	37	54	79	116	170	248	363	531	776	1135	1660	2427	3548	5188					
1.26	39	57	83	122	178	260	380	556	813	1189	1738	2541	3715	5432					
1.28	41	60	87	127	186	272	398	582	851	1245	1820	2661	3891	5689					
1.3	43	62	91	133	195	285	417	610	891	1303	1906	2786	4074	5957					
1.32	45	65	95	140	204	299	437	638	933	1365	1995	2917	4266	6237					
1.34	47	68	100	146	214	313	457	668	977	1429	2089	3055	4467	6531					
1.36	49	72	105	153	224	327	479	700	1023	1496	2188	3199	4677	6839					
1.38	51	75	110	160	234	343	501	733	1072	1567	2291	3350	4898	7161					
1.4	54	79	115	168	245	359	525	767	1122	1641	2399	3508	5129						
1.42	56	82	120	176	257	376	550	804	1175	1718	2512	3673	5370						
1.44	59	86	126	184	269	394	575	841	1230	1799	2630	3846	5623						
1.46	62	90	132	193	282	412	603	881	1288	1884	2754	4027	5888						

Figure 6. A portion of figure 3 where feasible *A. koninckii* lifespans could exist under the condition of a constant increase in instar duration. The colored borders represent different mortality regimes. See figure 3 for color key.

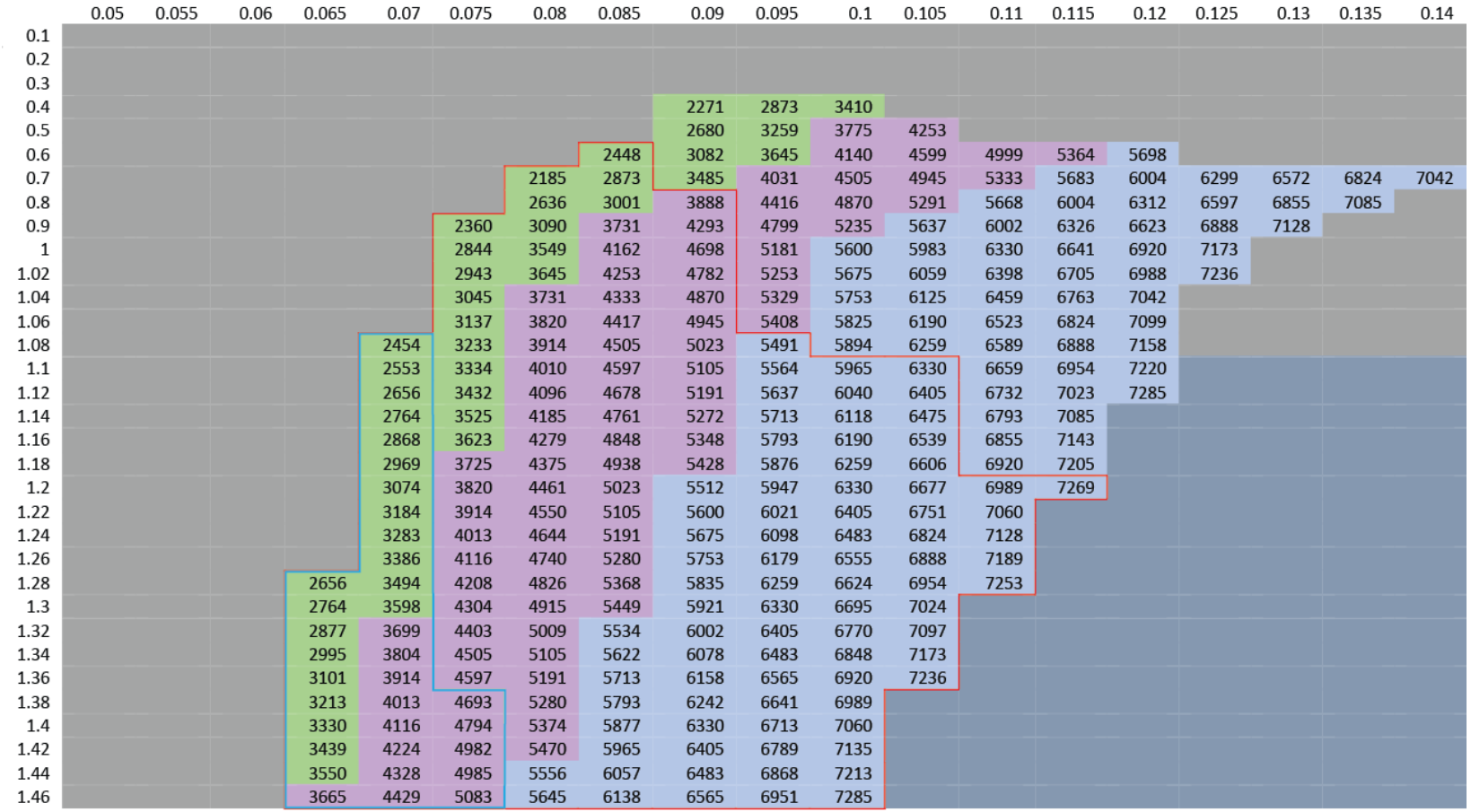

	0.05	0.055	0.06	0.065	0.07	0.075	0.08	0.085	0.09	0.095	0.1	0.105	0.11	0.115	0.12	0.125	0.13	0.135	0.14
0.1																			
0.2																			
0.3																			
0.4									2271	2873	3410								
0.5									2680	3259	3775	4253							
0.6								2448	3082	3645	4140	4599	4999	5364	5698				
0.7							2185	2873	3485	4031	4505	4945	5333	5683	6004	6299	6572	6824	7042
0.8							2636	3001	3888	4416	4870	5291	5668	6004	6312	6597	6855	7085	
0.9						2360	3090	3731	4293	4799	5235	5637	6002	6326	6623	6888	7128		
1						2844	3549	4162	4698	5181	5600	5983	6330	6641	6920	7173			
1.02						2943	3645	4253	4782	5253	5675	6059	6398	6705	6988	7236			
1.04						3045	3731	4333	4870	5329	5753	6125	6459	6763	7042				
1.06						3137	3820	4417	4945	5408	5825	6190	6523	6824	7099				
1.08					2454	3233	3914	4505	5023	5491	5894	6259	6589	6888	7158				
1.1					2553	3334	4010	4597	5105	5564	5965	6330	6659	6954	7220				
1.12					2656	3432	4096	4678	5191	5637	6040	6405	6732	7023	7285				
1.14					2764	3525	4185	4761	5272	5713	6118	6475	6793	7085					
1.16					2868	3623	4279	4848	5348	5793	6190	6539	6855	7143					
1.18					2969	3725	4375	4938	5428	5876	6259	6606	6920	7205					
1.2					3074	3820	4461	5023	5512	5947	6330	6677	6989	7269					
1.22					3184	3914	4550	5105	5600	6021	6405	6751	7060						
1.24					3283	4013	4644	5191	5675	6098	6483	6824	7128						
1.26					3386	4116	4740	5280	5753	6179	6555	6888	7189						
1.28				2656	3494	4208	4826	5368	5835	6259	6624	6954	7253						
1.3				2764	3598	4304	4915	5449	5921	6330	6695	7024							
1.32				2877	3699	4403	5009	5534	6002	6405	6770	7097							
1.34				2995	3804	4505	5105	5622	6078	6483	6848	7173							
1.36				3101	3914	4597	5191	5713	6158	6565	6920	7236							
1.38				3213	4013	4693	5280	5793	6242	6641	6989								
1.4				3330	4116	4794	5374	5877	6330	6713	7060								
1.42				3439	4224	4982	5470	5965	6405	6789	7135								
1.44				3550	4328	4985	5556	6057	6483	6868	7213								
1.46				3665	4429	5083	5645	6138	6565	6951	7285								

Figure 7. A portion of figure 4 where feasible *A. koninckii* lifespans could exist under the condition of a 365 day maximum instar duration. The colored borders represent different mortality regimes. See figure 3 for color key.

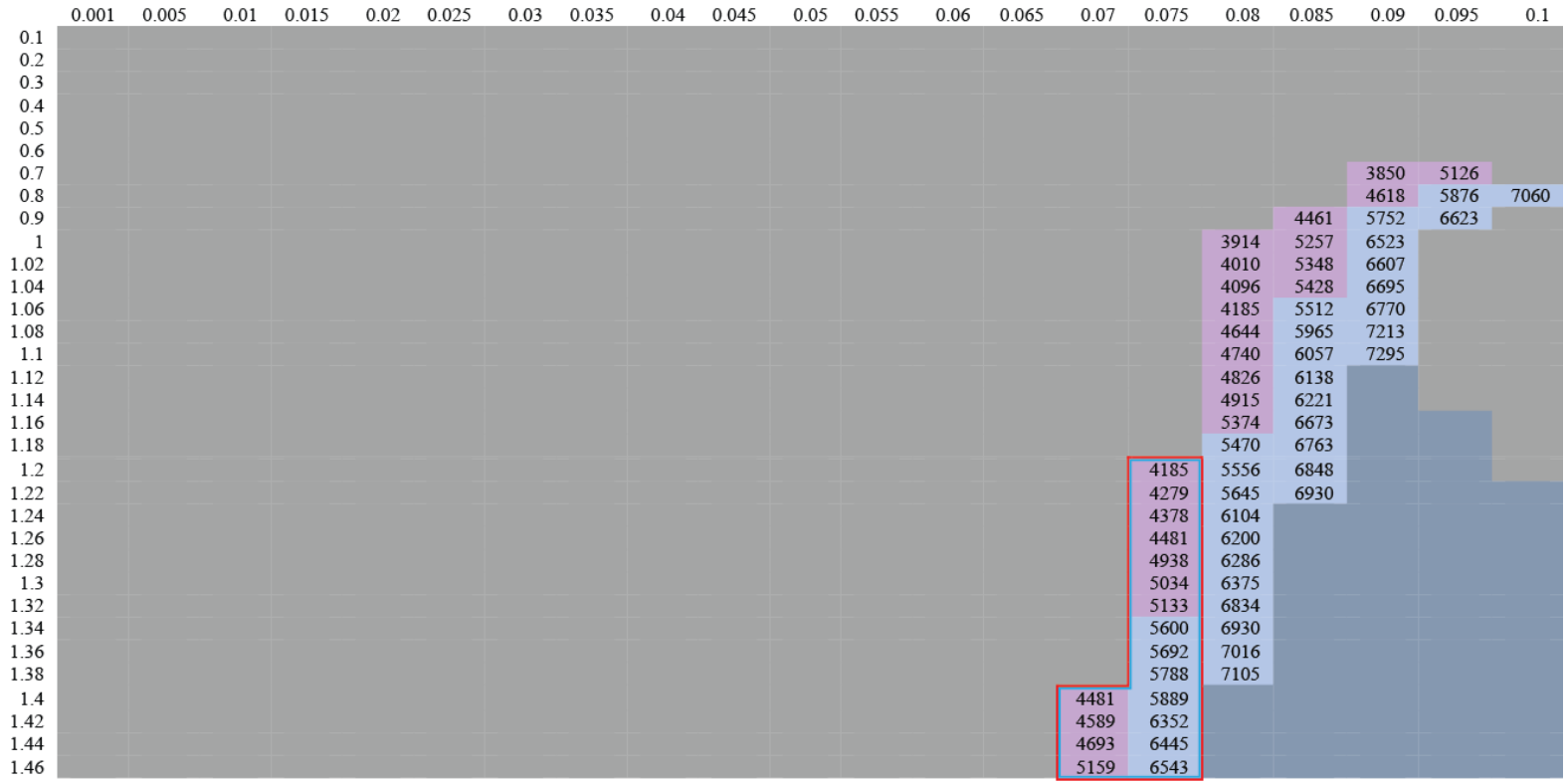

Figure 8. A portion of figure 5 where feasible *A. koninckii* lifespans could exist under the condition of a 730 day maximum instar duration. The colored borders represent different mortality regimes. See figure 3 for color key.

The total number of viable life spans in figures 6-8 are sorted by mortality rate and instar duration mode and binned into 5 year increments in Table 1. These numbers were then totaled in Table 2 by mortality rate.

Life Span total bins	0-5 Years	5-10 Years	10-15 Years	15-20 Years
Continuous Increase- 5%	313	54	30	19
Continuous Increase – 10%	294	38	12	2
Continuous Increase – 15%	270	10	0	0
365 Day Max- 5%	0	39	73	93
365 Day Max- 10%	0	21	14	0
365 Day Max- 15%	0	0	0	0
730 Day Max- 5%	0	0	11	7
730 Day Max- 10%	0	0	11	7
730 Day Max- 15%	0	0	0	0

Table 1: Total of viable life spans by life span mode and mortality regime

# of potentially viable life spans by bin	0-5 years	5-10 years	10-15 years	15-20 years
5%	313	93	114	119
10%	294	59	37	9
15%	270	10	0	0

Table 2: Total number of viable lifespans totaled per mortality regime by lifespan bin. Data compiled from Table 1.

Tables 1 and 2 show that as mortality increases the number of viable life spans decreases. In addition, that higher mortality regimes favor shorter life spans and therefore also short instar durations. By a 365 day maximum instar duration a 15% first meraspid instar mortality rate is no longer viable but does yield viable life spans under 10 years in total duration in a constant increase instar duration model. If mortality rates greater than 15% were to be applied these would only be viable at increasingly shorter instar durations and total life spans.

	Continuous Increase	365 Day Max	730 Day Max
5%	416	205	18
10%	346	35	18
15%	280	0	0
Total	1042	240	36

Table 3: Total Number of Viable Lifespans in each instar duration regime. Data compiled from Table 1.

Table 3 compiles the data from Table 1 by instar duration mode and mortality rate. As expected *A. koninckii* prefers a model with shorter durations, due to the 20 year maximum life span imposed on the data and the large number of instars.

General Shape of Frequency Distributions by Instar and Size

All life spans that were viable under a particular mortality regime, within a colored border in figures 6-8, and had a larval or protaspid phase of less than 30 days were run through the model to generate size frequency distributions. A general pattern emerged in the size frequency distributions produced in all three instar duration regimes. In all cases the corpses-only, exuviae-only, and corpses and exuviae plots were right skewed. However, the live population distributions differed greatly depending on both the duration of the instars and the mortality rate applied. For live populations normal distributions were the most common. Figures 9-14 show the variety of distributions that were produced over the range of data tested.

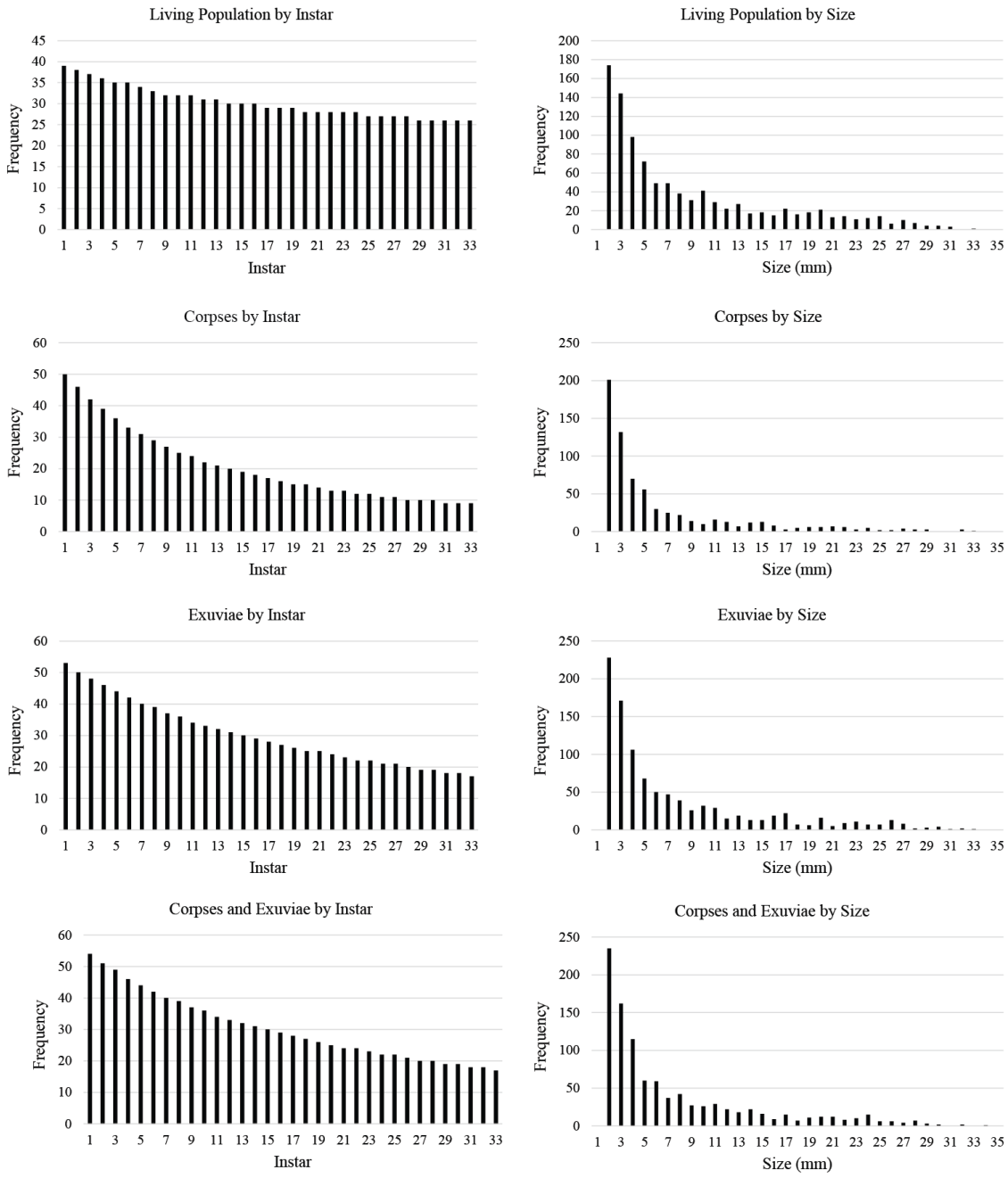

Figure 9- A series of frequency distributions from the Constant Increase/ .01/ 1.4 model.

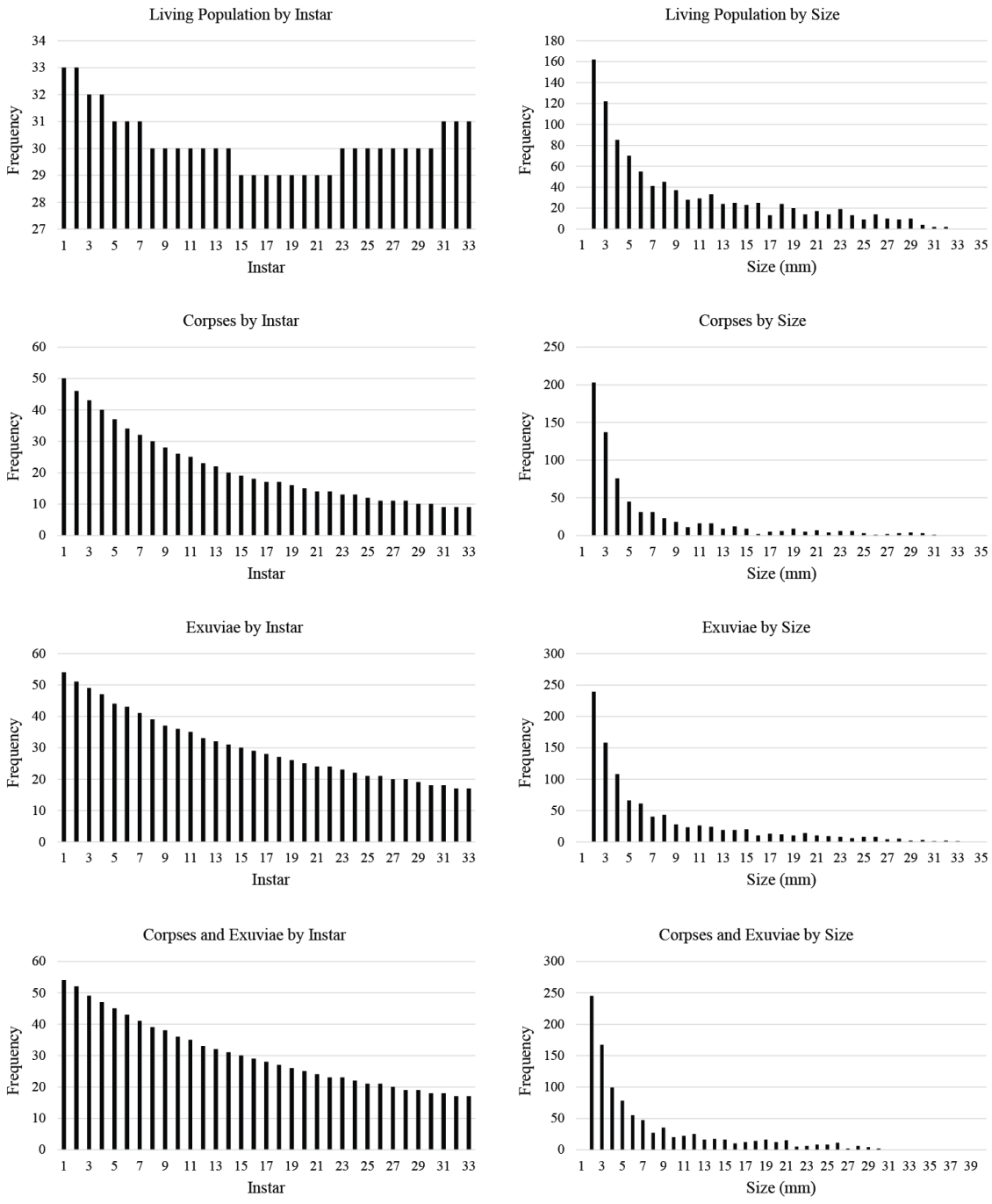

Figure 10- A series of frequency distributions from the Constant Increase/ .015/ 1.46 model.

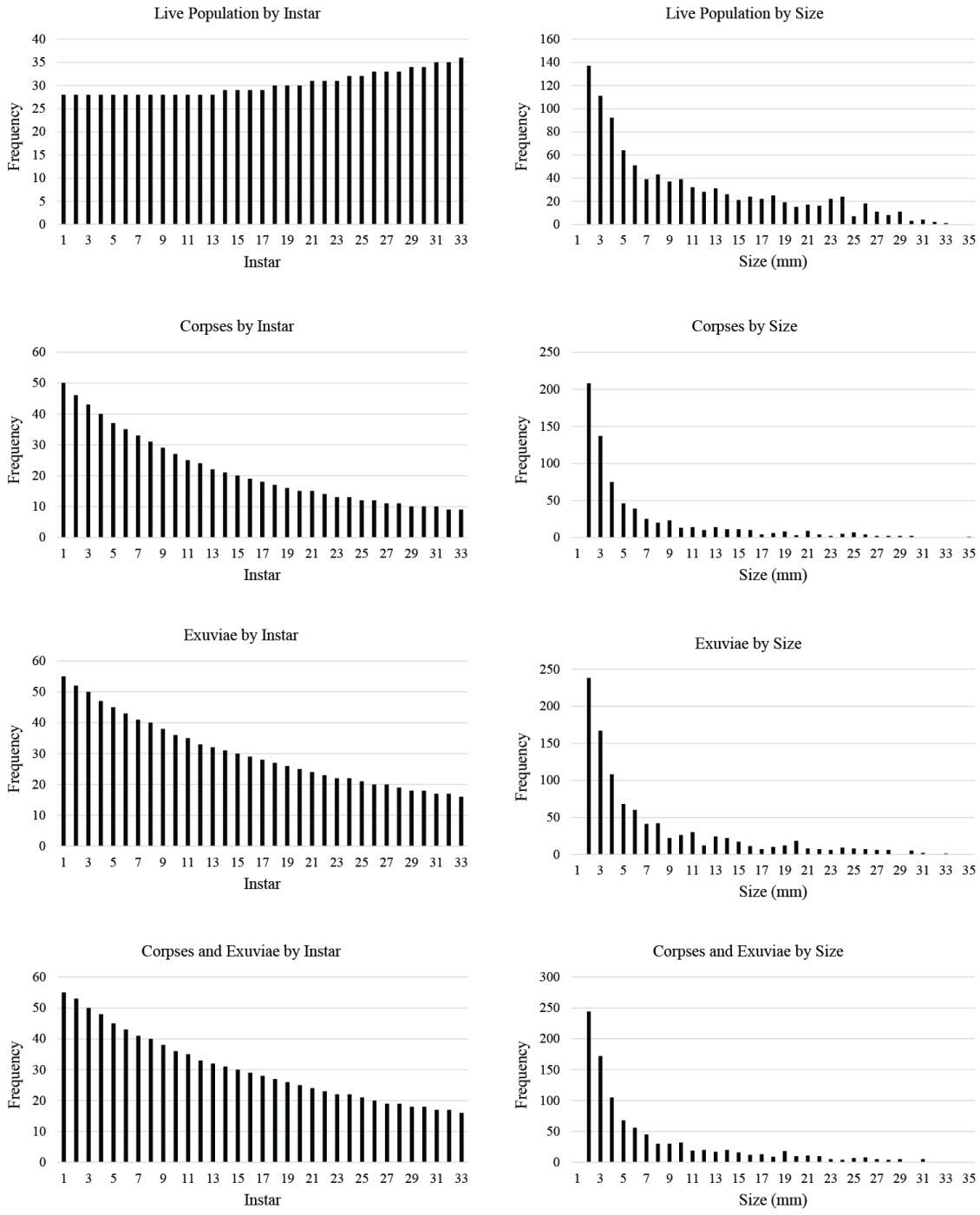

Figure 11- A series of frequency distributions from the Constant Increase/ .02/ 1.46 model.

Figures 9, 10, and 11, are typical of life spans that have short instar durations ranging from less than a day to a few days. Since these instar durations are short, mortality rates associated with intermolt mortality did not range far from the initial mortality rate given at the first meraspid instar. Typically these mortality rates only fluctuated within 5% of the given mortality rate. When calculating the mortality rate using the shortest durations (fractions of days) the mortality rate typically decreased as the instar number increased (Figure 9). As instar durations increase and mortality rates begin to differ on a larger scale (days) the live population frequency distribution by instar transitioned to a curve with maxima at both the early and late instars (Figure 10). This curve quickly transitioned in a linear increase in the number of individuals per instar (Figure 11).

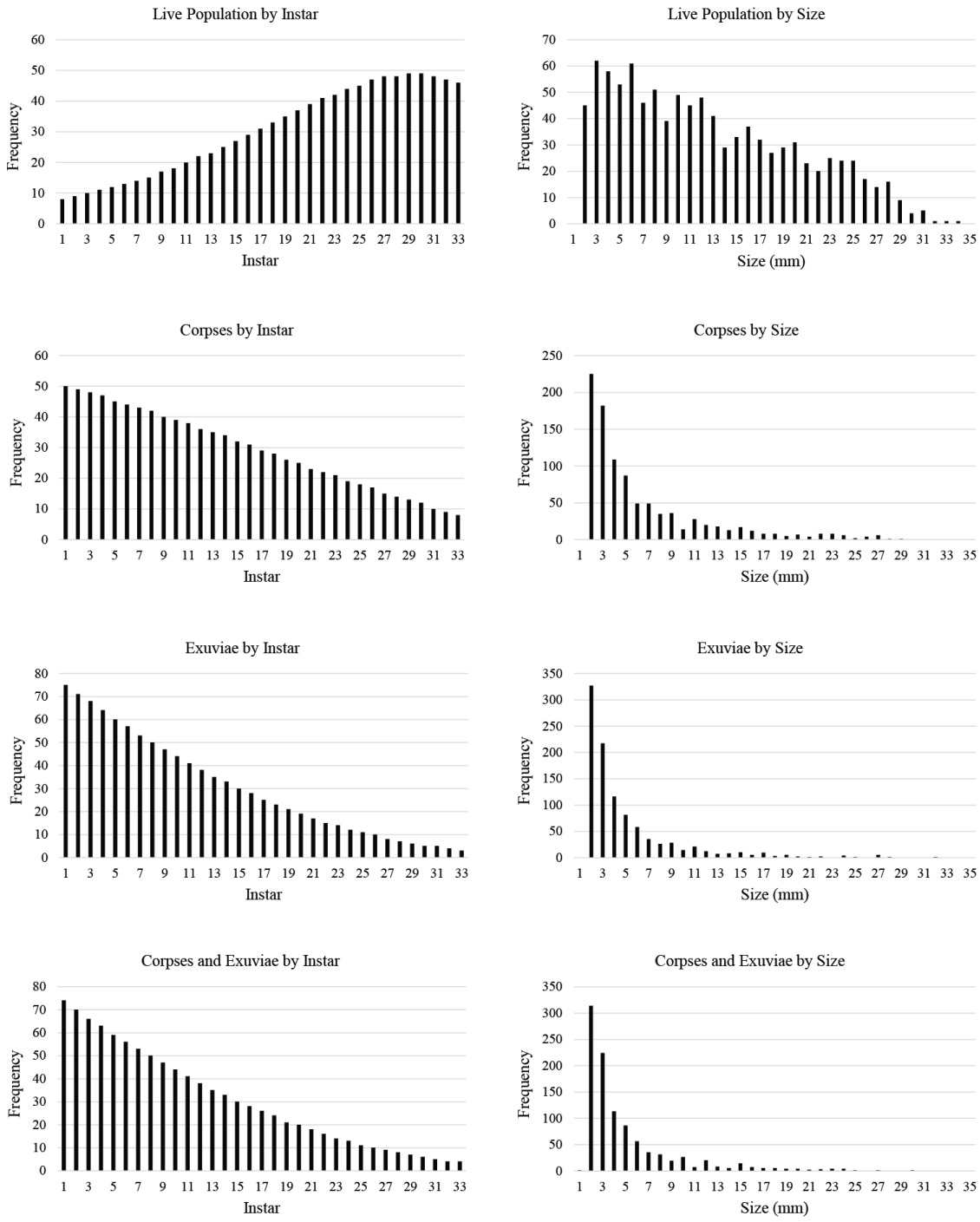

Figure 12- A series of frequency distributions from the Constant Increase/ .065/ 1.46 model.

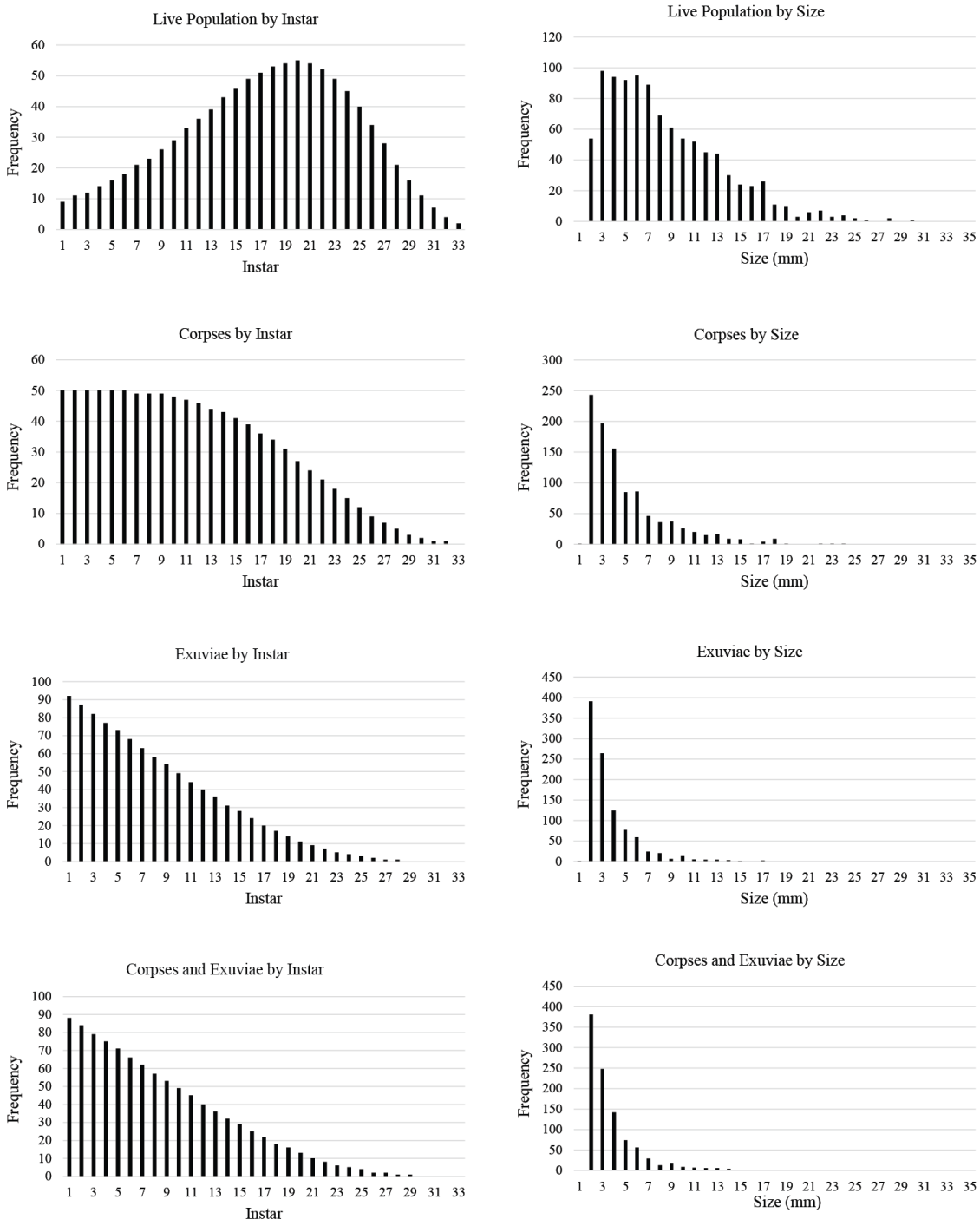

Figure 13- A series of frequency distributions from the Constant Increase/ .085/ .1 model.

More typical of the data were figures 12 and 13. Figure 12 exhibits a left skewed distribution while figure 13 shows a typical bell curve representing the live population. The bell curve, figure 13, is typically centered on the middle instars (i.e. instar 15-25) as those most commonly represented within live populations by instar distribution throughout all instar duration regimes and initial meraspid mortality rates. As stated for figures 9, 10, and 11 as both instar duration and differences in the length of instars durations increase the frequency distribution by instar transitions into a normal distribution.

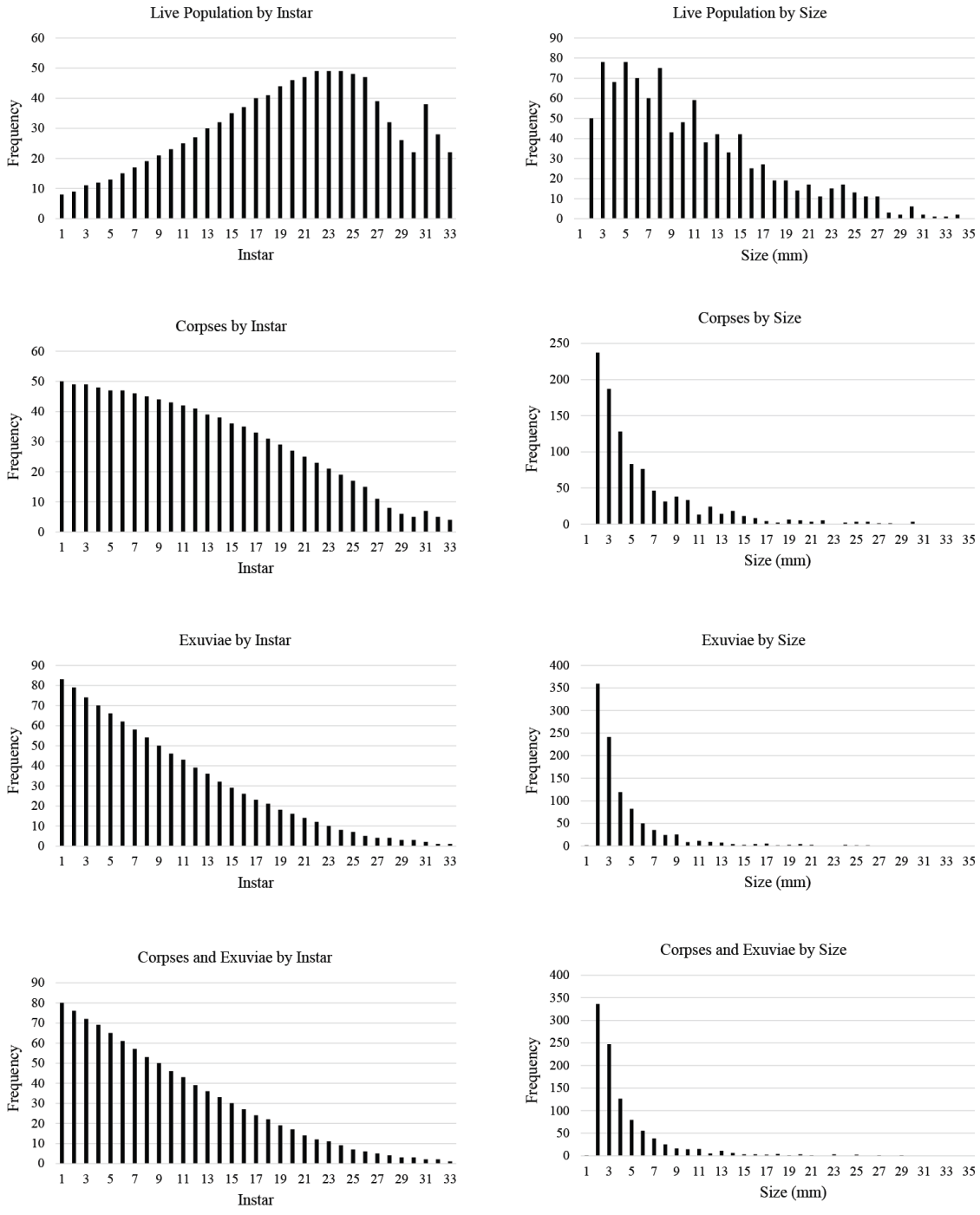

Figure 14- A series of frequency distributions from the 730 day maximum/ .075/ 1.4 model.

Figure 14 shows the effect of the scenario where a 730 day maximum instar duration is assumed for the latest stage instars. The increase in individuals towards the largest instars is a reflection of the change from a 365 day instar duration to a 730 day duration. While there is an increase in mortality between the two durations (about 10%) it is insufficient to counteract the large increase in instar duration which causes individuals inhabiting these instars to increase in number despite an increase in mortality.

Figures 9 through 13 show an overall trend in the shape of the live distributions due to the changing influence of intermolt mortality as the molt frequency declines. When instar durations are short (hours to days), changes in mortality rates between instars are small (fractions of a percentage). As the instar durations begin to increase in length (months to years) and therefore mortality rates between instars differ more (multiple percentage point changes between instars), a bell curve becomes the general trend of the live population per instar graphs. This occurs because as molting rate declines individuals of different ages begin to compound in the larger instars. While live population by instar graphs can differ greatly, the corpses, exuviae, and corpses and exuviae by instar and all distributions by size are all right skewed to varying degrees. There is little variation between all right skewed graphs in regards to general shape, which is in contrast to what is typically found in the fossil record (normal distributions).

Although Hartnoll and Bryant (1990) showed that it was possible to produce normal size frequency distributions in populations of living individuals assuming constant recruitment, invoking this to explain all approximately normal trilobite size frequency distributions is difficult to justify, except in cases in which there is some

indication that all exoskeletons preserved together represent a simultaneous, instantaneous kill of a standing population of individuals. In other cases, in which corpses or exuviae may form a significant component of the collection, interpreting a normal distribution as an unbiased natural sample is more difficult to justify. In such cases, this model forces us to consider other possibilities, such as a preservation bias against the preservation of smaller individuals as a possible cause for the approximately normal size frequency distributions observed. By applying such a bias, it is possible to produce approximately normal distributions in order to mimic distributions that are seen in the fossil record (Fig. 13).

Instar Number	Preservation Bias Corpses	Preservation Bias Exuviae
1	0.05	0.01
2	0.05	0.01
3	0.05	0.01
4	0.05	0.01
5	0.05	0.01
6	0.05	0.01
7	0.05	0.01
8	0.05	0.01
9	0.05	0.01
10	0.05	0.01
11	0.1	0.01
12	0.1	0.05
13	0.1	0.05
14	0.1	0.05
15	0.1	0.05
16	0.5	0.05
17	0.5	0.5
18	0.5	0.5
19	0.5	0.5
20	0.5	0.5
21	1	0.5
22	1	1
23	1	1
24	1	1
25	1	1
26	1	1
27	1	1
28	1	1
29	1	1
30	1	1
31	1	1
32	1	1
33	1	1

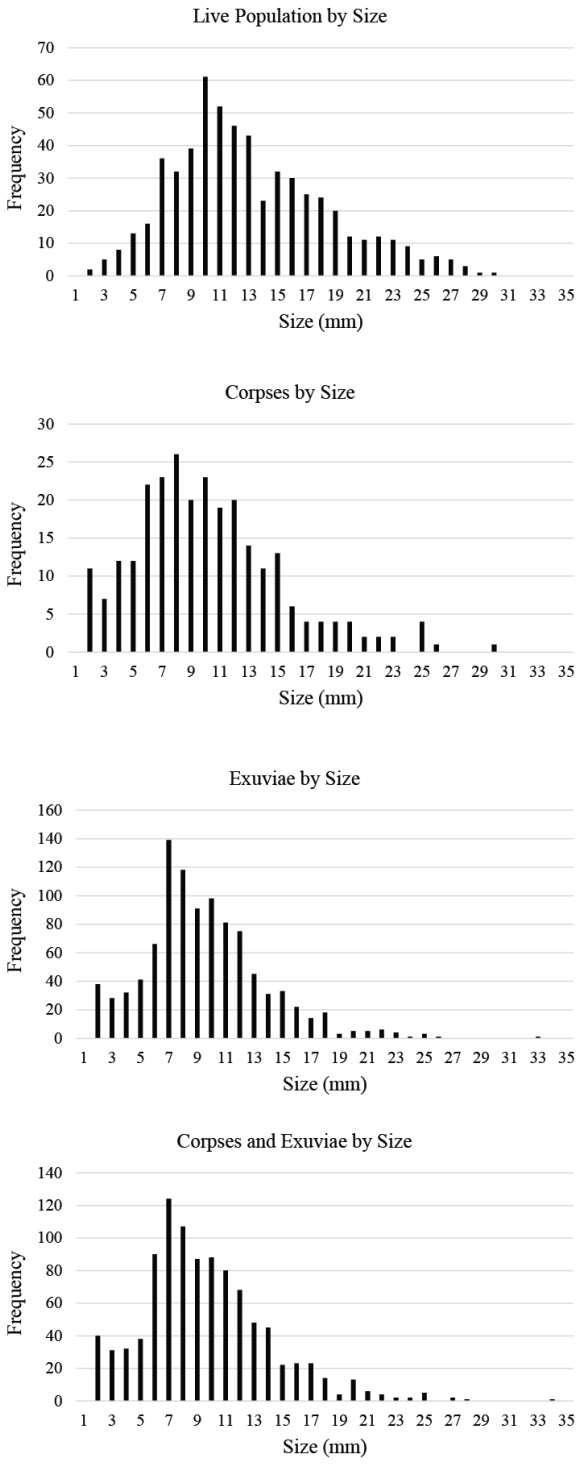

Figure 15- Distributions exhibiting a preservation bias on both corpses and exuviae. Preservation values per instar in table.

In figure 15, a value of 'one' represented 100% preservation, while those values smaller than one indicate the proportion of the individuals present in that instar that have been preserved. To produce the distribution seen in figure 15, a severe bias (1-5% of remains survive the fossilization process) had to be applied to early instars, and to slacken to zero in later ones, to create normal distributions. Size frequency distributions that incorporate exuviae need a larger preservation bias (only 1 to 5% of individuals preserved) compared to corpses (5-10% preserved). Each individual can potentially produce multiple exuviae but only one corpse. Therefore a larger preservation bias is needed to offset this difference in the production of individual entities.

Discussion

Assuming that molt duration did vary systematically on *A. koninckii* from the Na Cernidlech site according to the parameters of the general description of growth provided by Anderson and Ford (1976), this thesis shows it was possible to apply Hartnoll and Bryant's (1990) model to the observed data on *A. koninckii* to achieve individuals that reach the largest sizes observed among the thousands of trilobites recovered at the site.

Compared to most modern marine arthropods, *A. koninckii* has a large number of instars totaling 33 instars in its meraspid and holaspid phases while only reaching an average maximum size of about 27 mm. Under a model of progressively increasing intermolt periods, the occurrence of 33 instars places relatively strong constraints on the growth parameters possible.

Based on life span distributions that are considered viable given plausible durations of pre-meraspid stages and a total lifespan being less than a maximum of 20 years (Figures 6-8), *A. koninckii* could have had a life span that fit any three of the different instar duration trends exhibited among marine arthropods today. However, the results in table 3 suggest the widest range of plausible solutions for *A. koninckii*'s instar durations, followed the "constant increase" model in which intermolt duration was directly proportional to age, and did not stabilize in once per year or biannual patterns. Such an instar duration style is easier to envisage for species with relatively short life spans. It is possible that even the largest *A. koninckii* may not represent individuals that were older than 5 years at a maximum. On the other hand, at the shorter durations, it seems unlikely that this animal would have molted with frequencies of less than 40 minutes at its smallest instars, which would be required if total life spans less than 50 days.

Furthermore, assuming the growth model is applicable, the mortality of *A. konickii* must have been within the range of 5-10% mortality at the first meraspid instar in order for a portion of the population to reach the maximum size observed. Higher starting mortalities failed to produce frequency distributions in which all 33 instars were achieved. Compared to modern marine arthropods, 5-10% mortality is low but still reasonable in environment that *A. koninckii* lived. There is independent evidence that *A. koninckii* flourished in conditions of low oxygen. The lack of evidence of predation on the animal (Hughes et al., 2014) make low mortality a possibility. The beds that contain the *A. koninckii* assemblages vary in the mean size of articulated individuals but

invariably contain individuals that represented several different instars (Hughes et al., 2014); often ten or more instars are present. On the other hand, no bed has been observed in which material from most or all of the 33 instars is preserved. The presence of rare enrolled specimens shows that some animals were alive immediately prior to burial, but most other specimens are partially disarticulated. This means if catastrophic death had occurred it happened significantly prior to burial. The accumulations also include specimens with particular sclerite dispositions suggestive of exuviae.

Although dissolution of the original calcite makes it hard to distinguish the smallest specimens of *A. koninckii* from the matrix, the taphonomic filter modeled above evidently did not apply directly at the Na Cernidlech site because the site is famous for the common preservation of articulated meraspid specimens from meraspid degree 4 onwards, and particular bedding plane assemblages have notably different mean sizes. This is significant for the interpretation of those assemblages made up of holaspid (i.e. mature) individuals only; there are no correlated differences in substrate or other aspects of paleoenvironment to suggest a reduced likelihood of meraspid preservation within such assemblages. It does not seem plausible, therefore, to suggest that the reduced frequency of smaller specimens in these assemblages was the result of selective deletion of meraspids from the preserved record due to taphonomic causes. Rather, it seems that the exoskeletons were not permitted the chance to enter the record. The origin of such a pre-burial taphonomic filter is unclear. There is no evidence that smaller specimens were preyed upon i.e., fragmented (as opposed to cracked) fossils are absent from the assemblage. Furthermore, the distribution of small exuviae need not be expected to

mimic prey upon smaller live individuals, yet both are absent. Assemblages with common holaspid specimens also span a wide range of sizes, and therefore instars. If the model of decreasing molt rate at later size is correct, then these assemblages would include live individuals spawned over a considerable period of time. One explanation for the lack of smaller individuals might be that they were only preserved at the sediment-water interface for relatively short periods of time, longer than by removal by decay or dissolution. The absence of any smaller meraspids from these assemblages, which apparently did include both holaspid exuviae and carcasses, is curious and might imply a pattern of intermittent recruitment.

Based on particular patterns of sclerite disposition, the Na Cernidlech assemblage includes individuals alive at the time of burial; it is clearly not only a life assemblage (i.e. an assemblage of animals alive at the start of events that lead to their preservation), but also includes at least some exuviae. Hence the modeling leads to the expectation that the instars represented most commonly would be the smaller ones. In addition, when observing size frequency distributions on an arithmetic scale, a larger number of smaller trilobites are expected any size bin of a unit size will span more instars at smaller size than at larger size, unless a size-related adjustment is made to bin size. If the size bins are larger than in the growth increment per instar, at smaller sizes data from more than a single instar will be conflated into a standard sized bin. As distributions approximating normal distributions are the norm at Na Cernidlech, it seems inevitable that some kind of a preservation bias has to be invoked.

To recreate the types of size frequency distributions observed in the fossil record using a preservation bias, the bias must be applied the most heavily at the earlier instars, i.e., the smallest sized individuals. In some cases a preservation bias as high as 95 to 99% must be added to the earliest instars/ sizes (Figure 15) to produce data to having normal distributions. The causes of this preservation bias are unclear and could vary on a per assemblage basis. It should be acknowledged that a preservation bias is needed to achieve observed size frequency distributions.

The model used herein has significant limitations. Principal among these are: (1) the assumption of constant recruitment, which is inconsistent with opportunistic species such as *A. koninckii*, (2) the accuracy of the assumed mortality rates, (3) the assumption that the modeled changes in molt tempo derived from a modern arthropod applied to *A. koninckii*, and (4) the model may be biased towards longer lifespans. Limitation (2) likely has the least significance, unless mortality varies abruptly at one or more specific points in ontogeny for which there is little independent evidence. A marked change in exuviation style does occur at a characteristic size and might have implications for molt-related mortality. Limitation (1) is potentially significant, depending on the manner of variation in recruitment rate. A "boom and bust" or k-selective reproductive strategy might violate this limitation (Gould, 1977). I would expect the normal steady state size frequency distribution to deform into a series of pulsed peaks that collectively sum to a normal distribution. Assumption (3) is possibly the most difficult to evaluate for a fossil species, but it is relatively easy to model over a broad range of values. Anderson and Ford (1976) acknowledged that their equation for back or forward calculating instar

durations may be inaccurate due to the uncertainties and variation in decapod growth per instar. Hartnoll (1978) also recognized this variation, noting that water chemistry and temperature can significantly affect the growth rates and maximum size of individuals from the crab species, *Rhithropanopeus harrisii*. Due to the lack of opportunity to raise trilobites in a lab setting and to determine the water chemistry and temperature of their habitat due to time averaging and the 'incompleteness' of the fossil record, are unlikely ever to be able to tell how these parameters directly affected trilobite growth in the study.

Assumption (4) acknowledges there is a bias towards arthropods with longer life spans. Due to this model assuming constant recruitment accurate size frequency distributions for life spans ranging from less than to just over one year cannot be correctly calculated. If *A. koninckii* lived less than a year, only one generation should be observed in the live population. Therefore individuals could not be occupying all instars at any given time.

Conclusions

The model provides some constraints on the biology of *A. koninckii* if the assumptions made to create this model are broadly correct. *A. koninckii* may have grown through a style of continuously increasing instar durations with a life span that would have ranged from less than a year up to five years. *A. koninckii*'s individual instar durations would have been relatively short, ranging from less than a day to several months in length. Those with the shortest life span totals had very little difference in instar durations. Those with longer life spans had not only longer instar durations but

also larger differences in durations between successive instars. For *A. koninckii* to reach all 33 instars, it is likely that its total starting mortality for meraspid one would have been somewhere between 5-10%, which is a markedly low value. In particular, mortality at molting appears to have been unusually low for an arthropod. This would be consistent with independent evidence of a low predation pressure setting. As mortality rates increase, the range of plausible growth coefficients decreased, restricted to only those with very short total lifespans.

Regardless of model parameter scenarios, in the absence of a specified preservational bias, only certain live population models achieved a normal distribution. Since the majority of assemblages of articulated trilobite remains include carcasses and exuviae, and not just individuals alive at the time of burial, it appears necessary to invoke severe preservation bias as a general feature of the trilobite record. The frequency distributions for corpses, exuviae, or a combination of the two could achieve a normal distribution when high preservation biases were assigned to early instars, with preservation bias greater for exuviae compared to corpses due to the different numbers of entities any individual could potentially produce. In *A. koninckii* such preservation bias might include sclerite by decay or dissolution prior to burial. An alternative explanation might be highly sporadic recruitment of individuals: which remains unstudied. Hence additional models incorporating a wider range of parameters should be tested to see if *A. koninckii*'s attributes can produce size frequency distributions.

References

ANDERSON, W.R., & FORD, R.F. 1976. Early Development, Growth and Survival of the Yellow Crab, Cancer Anthonyi Rathburn (Decapoda, Brachyura) in the Laboratory. *Aquaculture* 7, 267–79.

CARMICHAEL, R.H., RUTECKI, D. & VALIELA, I. 2003. Abundance and Population Structure of the Atlantic Horseshoe Crab Limulus Polyphemus in Pleasant Bay, Cape Cod. *Marine Ecology Progress Series* 246, 225–39.

DYAR, H.G. 1890. The Number of Molts of *Lepidopterous* Larvae. *Psyche* 5,420–422.

FEIST, R., MCNAMARA, K.J., CRÔNIER, C., & LEROSEY-AUBRIL, R. 2008. Patterns of Extinction and Recovery of Phacopid Trilobites during the Frasnian–Famennian (Late Devonian) Mass Extinction Event, Canning Basin, Western Australia. *Geological Magazine* 146 (01), 12.

FUSCO, G., GARLAND, T., HUNT, G., & HUGHES, N.C. 2012. Developmental Trait Evolution in Trilobites. *Evolution* 66 (2), 314–29.

FUSCO, G., HUGHES, N.C., WEBSTER, M., & MINELLI, A. 2004. Exploring Developmental Modes in a Fossil Arthropod: Growth and Trunk Segmentation of the Trilobite Aulacopleura Konincki. *The American Naturalist* 163 (2), 167–83.

GOOGLE. 2015. Google Visualization API. Google. https://developers.google.com/chart/.

GOULD, S.J. 1977. *Ontogeny and Phylogeny*. Cambridge: Belknap Press of Harvard University Press.

HARTNOLL, R.G., & BRYANT, A.D. 1990. Size-Frequency Distributions in Decapod Crustacea - the Quick, the Dead, and the Cast-Offs. *Journal of Crustacean Biology* 10, (1), 14–19.

HARTNOLL, R.G. 1978. The Effect of Salinity and Temperature on the Post-Larval Growth of the Crab Rhithropanopeus Harrisii. In *Physiology and Behavior of Marine Organisms*, 349–58. Pergamon Press Ltd.

HARTNOLL, R.G. 1982. Growth. In *The Biology of Crustacra, Vol. 2: Embryology, Morphology, and Genetics*, L.G. Abele, 111–96. New York: Academic Press.

HUGHES, N.C., KŘÍŽ, J., & MACQUAKER, J.H.S, & Huff, W.D. 2014. The Depositional Environment and Taphonomy of the Homerian ‘Aulacopleura Shales’ Fossil Assemblage near Lodenice, Czech Republic (Prague Basin, Perunican Microcontinent). *Bulletin of Geosciences* 89 (2), 219–38.

KARIM, T.S., & WESTROP, S.R. 2002. Taphonomy and Paleoecology of Ordovician Trilobite Clusters, Bromide Formation, South-Central Oklahoma. *Palaios* 17 (4), 394–402.

MIT, INTEL CORP, & CHROMIUM AUTHORS. 2015. Node-Webkit. Computer Software. NW.js. Vers.0.12.3.MIT.Web. <https://github.com/nwjs/nw.js>.

POLTERMANN, M. 2000. Growth, Production and Productivity of the Arctic Sympagic Amphipod Gammarus Wilkitzkii. *Marine Ecology Progress Series* 193, 109–16.

SHAFIR, A. & FIELD, J.G. 2014. Population Dynamics of the Isopod Cirolana Imposita Barnard in a Kelp-Bed. *Crustaceana* 39 (2), 185–96.

SHELDON, P.R. 1988. Trilobite Size-Frequency Distributions, Recognition of Instars, and Phyletic Size Changes. *Lethaia* 21, 293–306.

STRONG, K.W., & DABORN, G.R. 1979. Growth and Energy Utilisation of the Intertidal Isopod Idotea Baltica (Pallas). *Journal of Experimental Marine Biology and Ecology* 41, 101–23.

Appendix A

Sample data run for the calculation of one instar duration and the mortality per instar. Column 1 is the instar number. Column 2 uses equation 1 to calculate the days after hatching an instar occurs and Column 3 subtracts the numbers from Column 2 to get an instar duration. Column 4 solves for the mortality using equation 2.

Instar Number	Days after Hatching	Instar Duration (Days)	Mortality
0	10		
1	12.02264	2.022644	10
2	14.4544	2.431753	10.46764
3	17.37801	2.923611	10.97777
4	20.89296	3.514953	11.53381
5	25.11886	4.225903	12.14039
6	30.19952	5.080653	12.80167
7	36.30781	6.108288	13.5221
8	43.65158	7.343778	14.30727
9	52.48075	8.829163	15.16262
10	63.09573	10.61499	16.09388
11	75.85776	12.76202	17.10861
12	91.20108	15.34333	18.21289
13	109.6478	18.44674	19.41493
14	131.8257	22.17785	20.72352
15	158.4893	26.66365	22.14689
16	190.5461	32.05675	23.69561
17	229.0868	38.54069	25.37979
18	275.4229	46.33611	27.21171
19	331.1311	55.70825	29.20311
20	398.1072	66.97605	31.36779
21	478.6301	80.52292	33.72033
22	575.4399	96.80985	36.45494
23	691.831	116.391	39.5237
24	831.7638	139.9328	42.89276
25	1000	168.2362	46.586
26	1202.264	202.2644	50.64058
27	1445.44	243.1753	55.08934
28	1737.801	292.3611	59.97107
29	2089.296	351.4953	65.32709
30	2511.886	365	62.18161
31	3019.952	365	57.19379
32	3630.781	365	52.64023
33	4365.158	365	48.48314
Sum		3539.296	